

Article

Deep Learning-Based Forest Fire Risk Research on Monitoring and Early Warning Algorithms

Dongfang Shang^{1,2}, Fan Zhang³, Diping Yuan^{2,*}, Le Hong⁴, Haoze Zheng⁵ and Fenghao Yang⁶

¹ School of Safety Engineering, China University of Mining and Technology, Xuzhou 221116, China; shangoriental@126.com

² Shenzhen Research Institute, China University of Mining and Technology, Shenzhen 518057, China

³ School of Computer and Information Engineering, Henan University, Kaifeng 475004, China; zhangfan@henu.edu.cn

⁴ School of Electrical Engineering, Shanghai Dianji Univeristy, Shanghai 201306, China; hongle.9910@163.com

⁵ Department of Public and International Affairs, City University of Hong Kong, Kowloon, Hong Kong; hzzheng6-c@my.cityu.edu.hk

⁶ School of Big Data and Internet, Shenzhen Technology University, Shenzhen 518118, China; 202002010129@stumail.sztu.edu.cn

* Correspondence: dpyuan2002@aliyun.com

Abstract: With the development of image processing technology and video analysis technology, forest fire monitoring technology based on video recognition is more and more important in the field of forest fire prevention and control. The objects currently applied to forest fire video image monitoring system monitoring are mainly flames and smoke. This paper proposes a forest fire risk monitoring and early warning algorithm, which integrates a deep learning model, infrared monitoring and early warning, and forest fire weather index. The algorithm first obtains the current visible image and infrared image of the same forest area, utilizing a smoke detection model based on deep learning to detect smoke in the visible image, and obtains the confidence level of the occurrence of fire in said visible image. Then, it determines whether the local temperature value of said infrared image exceeds a preset warning value, and obtains a judgment result based on the infrared image. It calculates again a current FWI based on environmental data, and determines a current fire danger level based on the current FWI. Finally, it determines whether or not to carry out a fire warning based on said fire danger level, said confidence level of the occurrence of fire in said visible image, and said judgment result based on the infrared image. The experimental results show that the accuracy of the algorithm in this paper reaches 94.12%, precision is 96.1%, recall is 93.67, and F1-score is 94.87. The algorithm in this paper can improve the accuracy of smoke identification at the early stage of forest fire danger occurrence, especially by excluding the interference caused by clouds, fog, dust, and so on, thus improving the fire danger warning accuracy.

Keywords: deep learning; forest fire; FWI; forest fire risk early warning



Citation: Shang, D.; Zhang, F.; Yuan, D.; Hong, L.; Zheng, H.; Yang, F. Deep Learning-Based Forest Fire Risk Research on Monitoring and Early Warning Algorithms. *Fire* **2024**, *7*, 151. <https://doi.org/10.3390/fire7040151>

Academic Editors: Demin Gao, Shuo Zhang and Cheng He

Received: 17 March 2024

Revised: 3 April 2024

Accepted: 8 April 2024

Published: 22 April 2024



Copyright: © 2024 by the authors. Licensee MDPI, Basel, Switzerland. This article is an open access article distributed under the terms and conditions of the Creative Commons Attribution (CC BY) license (<https://creativecommons.org/licenses/by/4.0/>).

1. Introduction

Forests are vital to human survival, as they provide a variety of ecosystem services, such as air and water purification, land protection, and biodiversity conservation. Looking at the resource data of China's forestry industry, China's forest coverage rate is only 16.55 percent, far below the global average of 27 percent, and per capita, forest resources account for only 20 percent of the global average. However, forests have been damaged by various human activities, especially forest fires. Forest fires are sudden, rapid, widespread, difficult to fight, and extremely harmful. Forest fires cause serious economic losses and human casualties, directly touching the forest industry's sustainable development and the national ecological security barrier.

Traditional forest fire monitoring mainly uses ground patrol, watchtowers, airplanes, and satellites for monitoring. Due to the constraints of weather and climate, technical level,

and monitoring operation costs, ground patrol, and satellite remote sensing technology cannot monitor and collect information related to the start of forest fires in real time. With the development of image processing technology and video analysis technology, forest fire monitoring technology based on video recognition has gained more and more attention in the field of forest fire prevention and control and has been widely used. The objects currently applied to forest fire video image monitoring system monitoring are mainly flames and smoke.

In smoke recognition, the focus is on the discovery, extraction, and analysis of smoke in visible images. In 2001, Jerome and Philippe [1,2] from France proposed a fast algorithm for complex motion extraction in small spatial envelopes based on the extraction of localized motions from a cluster analysis of points in a multidimensional time-embedded space for smoke recognition, and in 2002 they proposed the main criterion for smoke recognition by extracting pixel continuous dynamic envelopes from an image through an extraction of segmentation techniques for pixel continuous dynamic envelopes. In 2003, F. Gomez-Rodriguez [3] of the University of Seville proposed wavelet and optical flow-based computerized image processing techniques for monitoring fire spread; in 2004, Fernandes A M [4] of Portugal used neural network algorithms to monitor a small-scale forest fire experiment, using a neural network algorithm to automatically identify smoke features in LIDAR signals collected in the experiment, which improved the classification efficiency of smoke feature patterns and reduced the false alarm rate. References [5–14] performed smoke detection using motion detection, color, texture, contour, and spatio-temporal features, respectively. References [15–17] on the other hand, used a deep belief network and a deep confidence network for training to obtain a smoke recognition model, which improved the detection rate and reduced the number of false alarms. References [18–24] used a convolutional neural network (CNN) model and Resnet50 network for smoke detection. References [25,26] talk about Conditional Random Fields (CRFs) and Bi-directional Long and Short-Term Memory Networks (ABi-LSTM) applied to smoke recognition, respectively. Xuehui Wu et al. [27] from Southeast University proposed a stable AdaBoost (RAB) classifier to improve the detection effect and performance of fire smoke detectors, and later proposed a new regularization and variable selection method. Reference [28] used the method of co-training a smoke recognition model with synthetic and real smoke images to improve the accuracy of smoke recognition. References [29–31] proposed some algorithms for forest fire detection, especially for how to improve accuracy in foggy environments.

In flame recognition, the main research focus is to optimize and improve the flame foreground, including the segmentation of the front and back view, the spatial and temporal features of the flame, and the recognition of the texture. Celik and Habiboglu et al. [32,33] in Turkey proposed to improve the flame detection effect by refining the classification of fire image elements and spatial and temporal features through statistical modeling, respectively. In 2019, Tan Yong et al. [34] at Jiangnan University improved the accuracy and anti-jamming performance of flame recognition using symbiotic matrices and an improved probabilistic neural network (PNN) method. Sun Xiaofang and Wu Xuehui [35,36], respectively, improved the support vector machine and applied it to flame recognition. Dai et al. [37] proposed a deep-learning-based multi-scale video flame detection model for fire warning, which solves the problem of weak and inconvenient detection of fire at an early stage.

The recognition of infrared images in conjunction with visible images plays an increasingly important role in forest fire monitoring and early warning technologies. In 2021, Ciprián-Sánchez et al. [38] proposed a deep-learning-based infrared-visible image fusion method, FIRE-GAN, for recovering areas occluded by smoke and haze. In 2021, Sun Fei et al. [39] utilized infrared and visible light bands to obtain composite feature information of forest fires using a binocular vision method. In 2022, Bowen Wang et al. [40,41] from Nanjing University of Science and Technology realized high-resolution infrared and visible light image reconstruction, which significantly improves the imaging quality of a fused image.

In summary, forest fire monitoring is mainly for flame image and smoke recognition. When a forest fire risk appears in the early stage, the flame is too small to be easily obscured

by the forest trees and cannot be monitored; when the flame is large enough to be recognized and monitored, the fire has spread to a certain scale, which makes it difficult to fight. Smoke recognition can be found in the early stage of a forest fire if the forest fire occurs in the early stage of the early warning, which can reduce the difficulty of fighting the fire and reduce the loss of life and property. However, fire-induced smoke is very similar to water mist, dust, and clouds, and the existing methods cannot distinguish them well, resulting in a high rate of misidentification. Therefore, how to improve the accuracy of smoke recognition in the early stage of forest fire, so as to improve the accuracy of fire warning is a technical problem that needs to be solved urgently.

2. Methodologies

In this paper, we propose a forest fire risk monitoring and early warning algorithm, which aims to improve the accuracy of smoke recognition in the early stage of forest fires, especially to differentiate between water mist, dust, clouds, and other situations that are prone to causing false alarms (see Figure 1), so as to improve the accuracy of early warning.

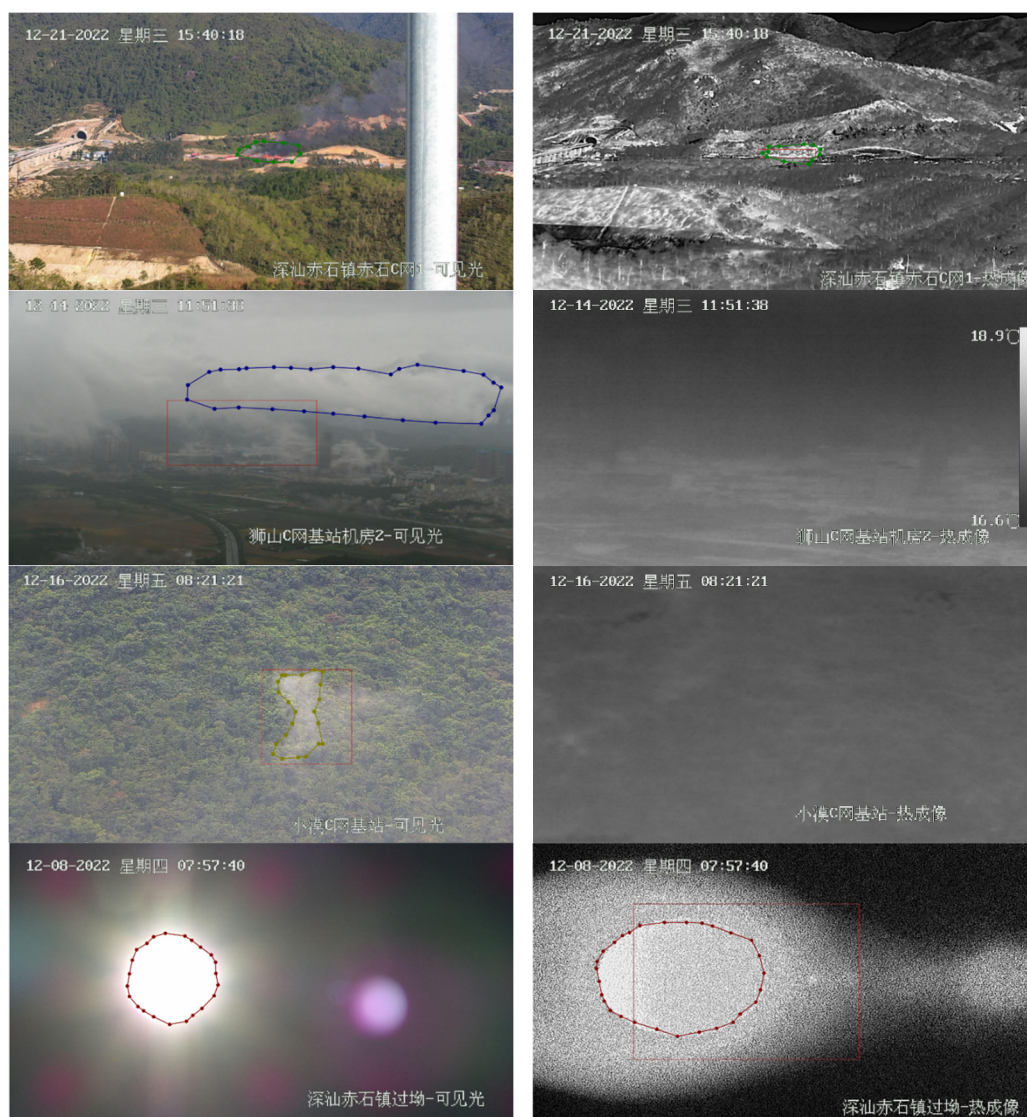


Figure 1. Visible and infrared images of pyrotechnics, clouds, fog, and the sun, from top to bottom.

The algorithm acquires a currently visible light image and an infrared image of the same forest area by means of a visible infrared bispectral camera. It firstly utilizes a smoke detection model based on deep learning to perform smoke detection on said visible light

image, and obtains the confidence level of the occurrence of fire in the said visible light image; secondly, it determines whether the local temperature value of said infrared image exceeds the preset warning value, and obtains the judgment result based on the infrared image. It then calculates a current FWI from which to determine the current fire danger level; and finally, it determines whether to issue a fire warning based on said fire danger level, said confidence level of the occurrence of fire in said visible light image, and said judgment result based on the infrared image. The algorithm flow is shown in Figure 2.

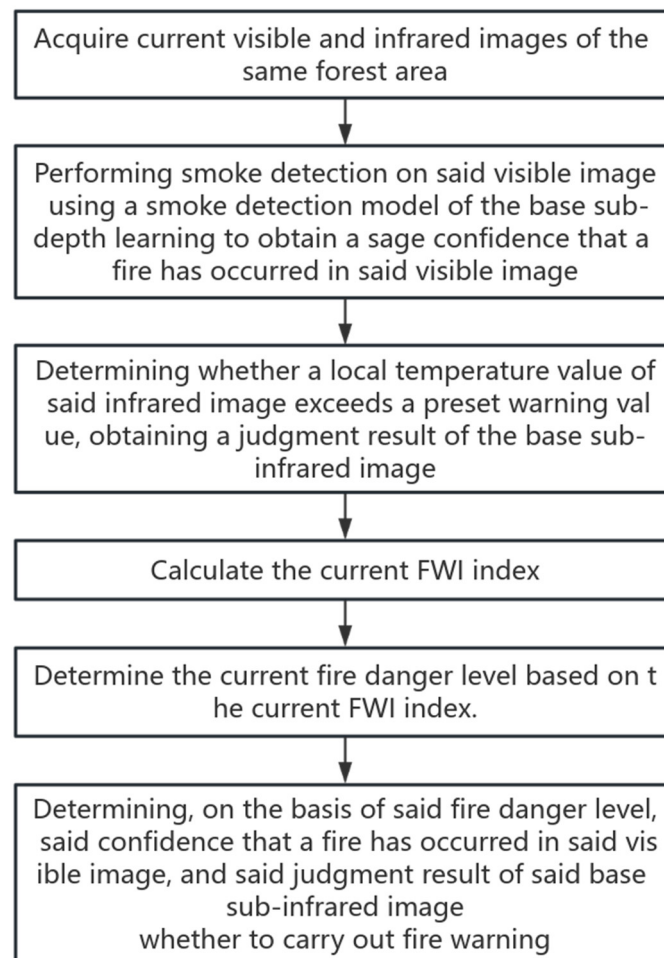


Figure 2. Flowchart of the algorithm in this paper.

2.1. YOLOv5 Training Model

The smoke detection model based on deep learning is pre-trained to obtain and specifically label the collected visible light images of the early stage of the forest fire, labeling the location and shape of the real fire point and the smoke and fire, and labeling the collected visible light images of other objects that can cause fire misreporting, such as fog images, cloud images, machine high temperature images, lake reflections, and building chimneys, etc. It also labels the other objects that can cause false alarms in the visible light images collected, including the location and shape of the object, such as clouds, fog, and dust, etc. Labeling is divided into four categories, namely, fire, clouds, fog, and other, and detecting smoke is the goal. Labeled images have been used to train the pre-programmed model, and ultimately program the training model to be able to detect smoke. The output of the model is the confidence level of fire occurrence in the input image. The confidence level that a fire has occurred in the input image should be interpreted as the confidence level that a fire has occurred in the actual environment corresponding to the input image.

Instead of viewing an image thousands of times (extracting thousands of Anchor Boxes) to produce a classification result, the YOLO family of object detection models transforms the object detection problem into a regression problem, using a deep neural network to predict object information and directly generate coordinates and probabilities for each category. During training, it processes the entire image at once, and its predictions are determined by the global context of the image. Thus, YOLO is an end-to-end single-stage approach that has been developed into several versions through continuous optimization to date [42,43].

YOLOv5 adopts weighted NMS in the screening of prediction frames, which also further improves the model prediction ability, so in this paper, YOLOv5 is selected for deep learning training on visible light images. The EMA attention mechanism is introduced in the model feature extraction network to improve the feature representation capability of the network, and the network model framework used in this paper is shown in Figure 3.

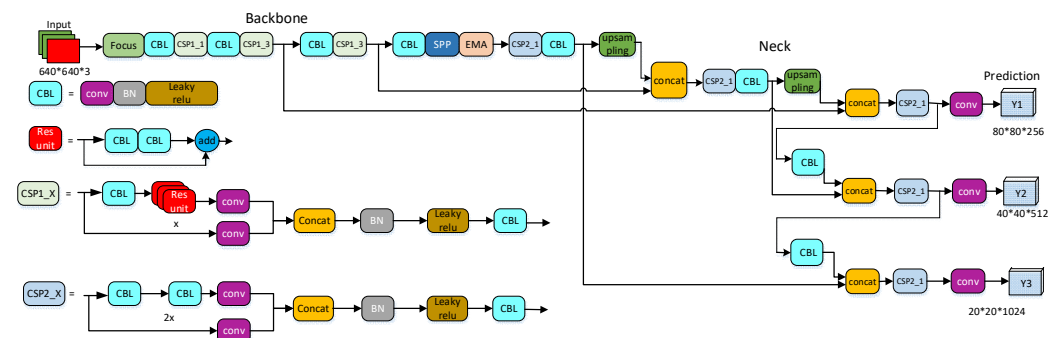


Figure 3. Structure of smoke detection model based on improved Yolov5.

Among them, the computational flow of the EMA attention mechanism [44] is shown in Figure 4, which fully considers the feature grouping and multi-scale structure, which is conducive to the effective establishment of short-term and long-term dependencies, thus obtaining better performance.

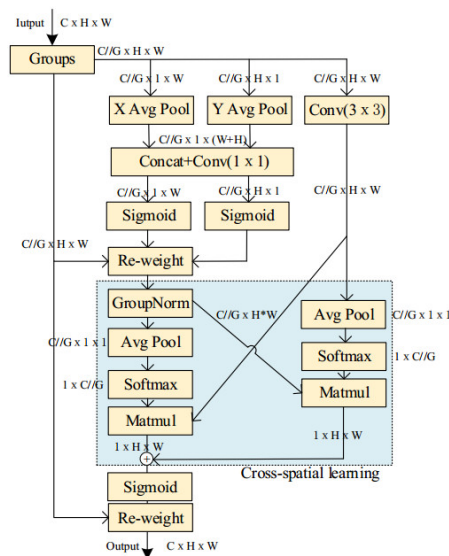


Figure 4. EMA attention mechanism calculation flowchart.

The module extracts the attention weight descriptors of the grouped feature map through three parallel routes. Two 1D global average pooling operations are employed to encode the channels along two spatial directions, respectively, in the 1×1 branch, and

only one 3×3 kernel is stacked in the 3×3 branch to capture the multiscale feature representation. After decomposing the output of the 1×1 convolution into two vectors, two nonlinear Sigmoid functions are utilized to fit the 2D binomial distribution after linear convolution. In order to achieve different cross-channel interaction features between the two parallel paths of the 1×1 branch, the two-channel smart attention maps within each group are aggregated together by multiplication. The 3×3 branch captures the local cross-channel interactions by a 3×3 convolution in order to expand the feature space. Inter-channel information is encoded to adjust the importance of different channels, and precise spatial structure information is retained in the channels. The global spatial information of the 1×1 branch outputs is encoded using 2D global average pooling. Finally, the output feature mapping within each group is computed as the set of the two spatial attention weight values generated, and then a Sigmoid function is used to highlight the global context of all pixels. Cross-spatial information aggregation methods are considered, and the parallel use of 3×3 and 1×1 convolutions allows for more contextual information to be utilized in the intermediate features, modeling remote dependencies while embedding precise location information into the EMA mechanism.

2.2. Infrared Thermal Imaging Early Warning

Infrared thermal imaging technology uses the reception of infrared radiation emitted by the object, and turns the measured target object surface infrared radiation into a video signal, while the detected target itself radiates heat energy, which will be converted into a real-time object surface reflecting the characteristics of the target thermal image, both to obtain the measured target temperature distribution to determine the state of the object. The background temperature of a forest area is generally -40 degrees to 60 degrees, while the temperature of the flame produced by forest combustible material is 600 to 1200 degrees; the temperature difference between the two is large, so the heat source can be detected as early as possible, so as to fulfil the purpose of preventing fires.

The temperature at the location of a burning or shaded fire point will be much higher than the surrounding temperature, so temperature characterization is preferred for fire identification and is the main reason for converting visible cameras to infrared cameras in forest fire monitoring and early warning methods. If the local temperature value of an infrared image exceeds the preset warning value, then it is considered that the forest area corresponding to the infrared image is very likely to contain a fire. When the local temperature value of the infrared image exceeds the preset warning value, the judgment result is recorded as 1. When the local temperature value of the infrared image does not exceed the preset warning value, the judgment result is recorded as 0.

2.3. Canadian Forest Fire Weather Index

Forest fires have a very close relationship with meteorological conditions. The main meteorological elements that have a significant impact on the occurrence and spread of forest fires are temperature, precipitation, relative humidity, wind speed, and so on.

The Canadian Fire Danger Rating System (CFFDRS) was developed by the Canadian Federal Forest Service in 1968, but initial research dates back to the 1820s. The two main subsystems of the CFFDRS, the Fire Weather Index (FWI) system, and the Fire Behavior Prediction (FBP) system, have been in official operation for many years; the other two subsystems, the Combustible Moisture Aid (CMA) system, and the Canadian Forest Fire Occurrence Prediction (FOP) system, are available in a variety of regional versions but are not available to the general public. Various regional versions exist, but they have not yet been developed into a national version [45].

The formulas for calculating the component factors of the FWI system can be found in the Equations and FORTRAN program for the Canadian Forest Fire Weather Index System [46] and the Development and structure of the Canadian forest fire weather index system [47]. Two books with detailed instructions.

In forest fire ecological studies, the Fire Weather Index (FWI) is the main indicator for predicting the occurrence of forest fire behavior, energy release, and estimating the size of fire danger, which can better reflect the fire weather conditions. The five-level system is commonly used in forest areas in China, where fire danger weather levels are categorized into five levels; see Table 1 for details.

Table 1. Fire Weather Index FWI values.

Rank	Name	Danger Degree	Flammability	Spread Degree	Color
First stage	Low fire risk	Lower	Difficult	Difficult	Green
Second stage	Lower fire risk	Relatively low	Relatively difficult	Relatively difficult	Blue
Third stage	Higher fire risk	Relatively high	Relatively easier	Relatively easier	Yellow
Fourth stage	High fire risk	High	Easy	Easy	Orange
Fifth stage	Very high fire risk	Extremely high	Extremely easy	Extremely easy	Red

2.4. Forest Fire Risk Early Warning Algorithm

The process of determining whether or not to issue a fire warning based on the fire danger level described earlier, the confidence level that a fire has occurred in the visible image, and the results of the infrared image-based judgment considers the following rules:

If the fire danger level is at level 2, and the confidence level of the visible light image of the occurrence of fire is greater than or equal to the first threshold value and the judgment result based on the infrared image is 1, then a fire warning is issued, wherein the judgment result based on the infrared image is 1, indicating that the local temperature value of said infrared image exceeds the warning value;

If the fire danger level is at level 3, and the confidence level of the occurrence of fire in the visible image is greater than or equal to the second threshold value and the judgment result based on the infrared image is 1, then a fire warning is issued;

If the fire danger level is at level 4, and the confidence degree of the occurrence of fire in the visible light image is greater than or equal to the third threshold value and the judgment result based on the infrared image is 1, a fire warning is issued;

If the fire danger level is at level 5, and the confidence level of the occurrence of fire in the visible light image is greater than or equal to the fourth threshold value and the judgment result based on the infrared image is 1, then a fire warning is issued, wherein said first threshold value is greater than said second threshold value, said second threshold value is greater than said third threshold value, and said third threshold value is greater than said fourth threshold value;

In other cases, no fire warning is issued.

This method is intended to improve the accuracy of fire warnings. Specifically, if the fire danger level is at level 2, and the confidence level of the occurrence of in the visible image is greater than or equal to the first threshold value and the judgment result based on the infrared image is 1, then it is determined that the recognized smoke is smoke generated by a fire, and a fire warning is issued, wherein the judgment result based on the infrared image is 1, indicating that the local temperature value of said infrared image exceeds the warning value. If the fire danger level is at level 3, and the confidence degree of the occurrence of fire in said visible light image is greater than or equal to the second threshold value and the judgment result based on the infrared image is 1, then it is determined that the recognized smoke is smoke generated by fire, and a fire warning is issued. If the fire danger level is at level 4, and the confidence degree of the occurrence of fire in the visible light image is greater than or equal to the third threshold value and the judgment result based on the infrared image is 1, then it is determined that the recognized smoke is fire-generated smoke, wherein a judgment result of 1 indicates that the local temperature value of said infrared image exceeds the warning value, and a fire warning is issued. If the fire danger level is at level 5, and the confidence level of the occurrence of fire in said visible light image is greater than or equal to the fourth threshold and the judgment result

based on the infrared image is 1, then it is determined that the recognized smoke is smoke generated by a fire, and a fire warning is issued. In addition to the above cases where a fire warning is required, a fire warning is not issued in other cases, i.e., smoke corresponding to other cases is not fire-generated smoke, e.g., when the fire danger level is 1, the recognized smoke is not fire-generated smoke, and a fire warning is not issued. That is, regardless of the value of the confidence level and the judgment result based on the infrared image, as long as the fire danger level is at level 1, a fire warning is not issued. Furthermore, for a case in which the fire danger level is at level 2, the confidence level of the occurrence of a fire in the visible image is greater than or equal to the first threshold value, and the judgment result based on the infrared image is 0, a fire warning is not issued. Table 2 shows the cases in which a fire warning is required, wherein a warning result of 1 indicates that a fire warning is required.

Table 2. Judgment rules of forest fire risk warning algorithm.

Fire Risk Level	1	2	3	4	5
Visible image confidence		≥90%	≥82%	≥65%	≥58%
Infrared warning		1	1	1	1
Early warning results	0	1	1	1	1

3. Results

3.1. Experimental Data

A 45-channel visible–infrared bispectral camera deployed in a certain area is selected, and the parameters of the camera are as follows: maximum image size: 640 × 512; focal length (lens): 100 mm; furthest fire point detection distance (based on 2 m × 2 m): 6000 m; furthest smoke detection distance (based on 5 m × 5 m): 8 km; field of view: 24.6° × 19.8°~6.2° × 5.0°; visible lens: 15.6–500 mm; support optical fog transmission; 360° continuous rotation in the horizontal direction, −45°~+45° in the vertical direction; power supply: DC48V; operating temperature and humidity: −40 °C to 65 °C, humidity less than 90%; protection grade: IP66.

The experimental images in this paper are all derived from natural camera shots, using 1359 visible light images captured in March and April 2023 and 1359 infrared images captured simultaneously to cover the four types of images that tend to trigger alarms. As shown in Figures 5–8.

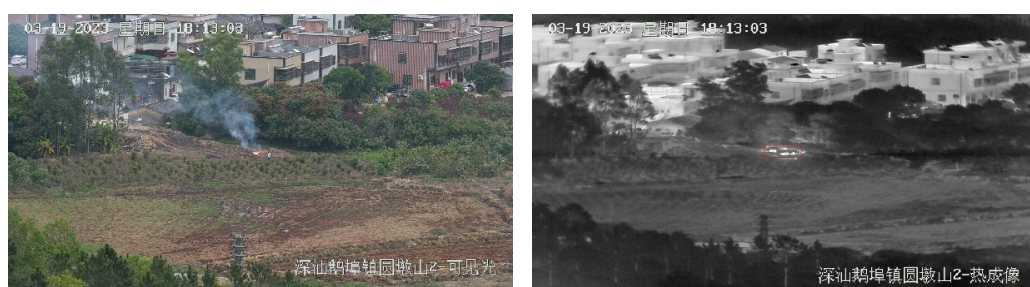


Figure 5. Image of smoke at the beginning of the fire.



Figure 6. Fog image.



Figure 7. Sun reflection image.

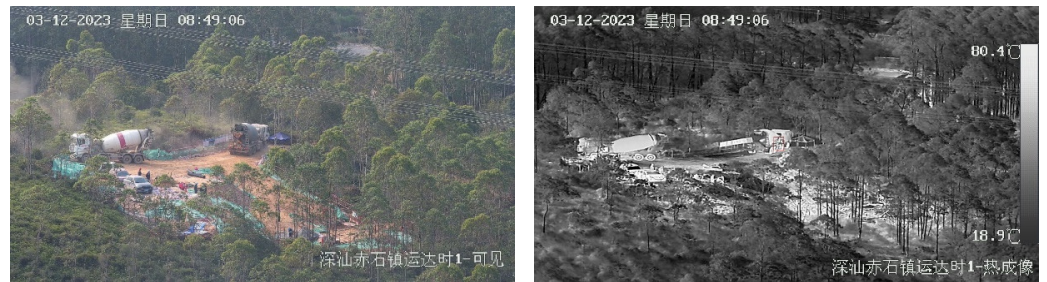


Figure 8. High temperature image of the machine.

The scenarios in which an infrared image warning is triggered are shown in Figures 9–12 respectively:



Figure 9. Visible and infrared maps of smoke.



Figure 10. Visible and infrared maps of lake reflections.



Figure 11. Visible and infrared plots of machine high temperatures.

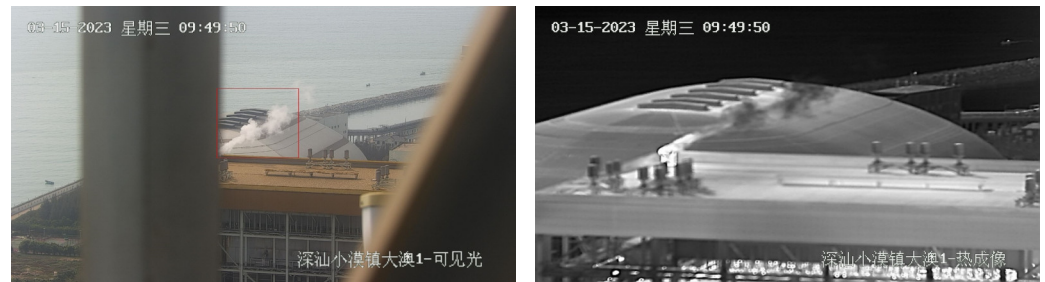


Figure 12. Visible and infrared maps of building chimneys.

3.2. Model Training

In this paper, we use the PyTorch deep learning framework, python 3.9 programming language, Windows 10 system, and NVIDIA Geforce Quad P6000 24 G video memory. The official pre-training weights of YOLOv5s are used, the number of training iterations is set to 600 epochs, the size is 16, the optimizer is SGD, the initial learning rate is 0.01, the momentum is 0.937, the regularization coefficient of weight decay is 0.005, and Mosaic is used for data enhancement.

In the article, 1359 visible image datasets are allocated according to the ratio of the training set, validation set, and test set, 8:1:1, of which 1088 are in the training set, 135 are in the validation set, and 136 are in the test set. The loss values and validation accuracy curves during training are shown in Figures 13 and 14.

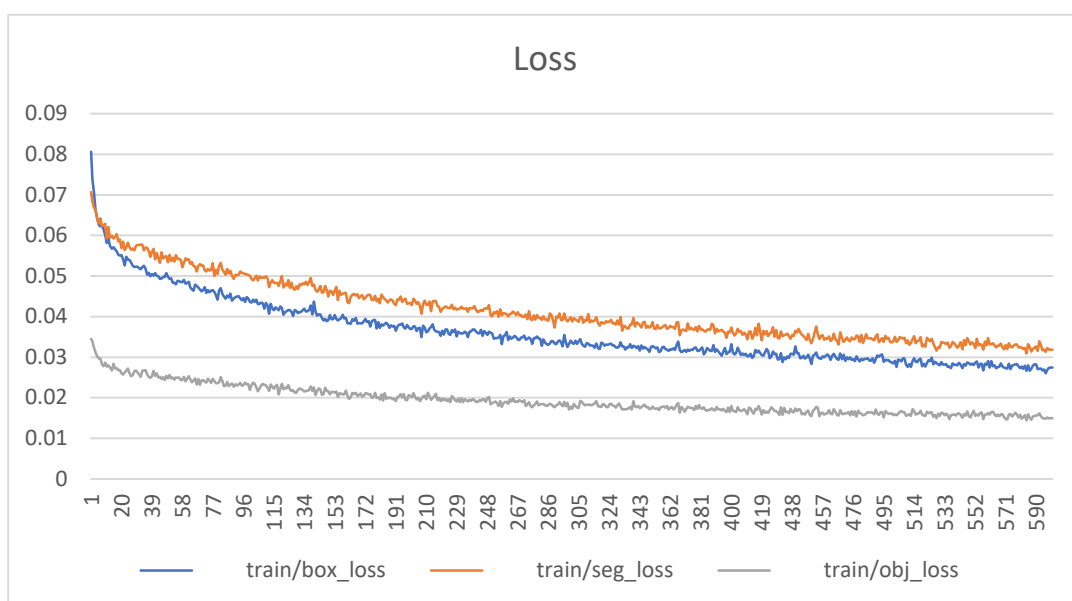


Figure 13. Model training loss value.

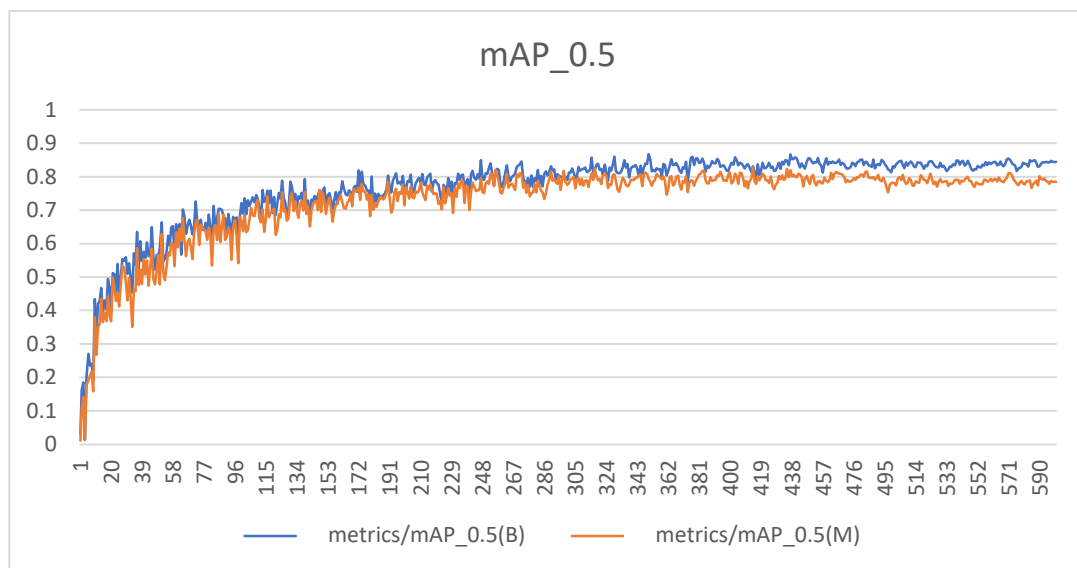


Figure 14. Model validation accuracy (mAP) comparison.

The PR curves for the test result data obtained from the model test set in this paper are shown in Figure 15:

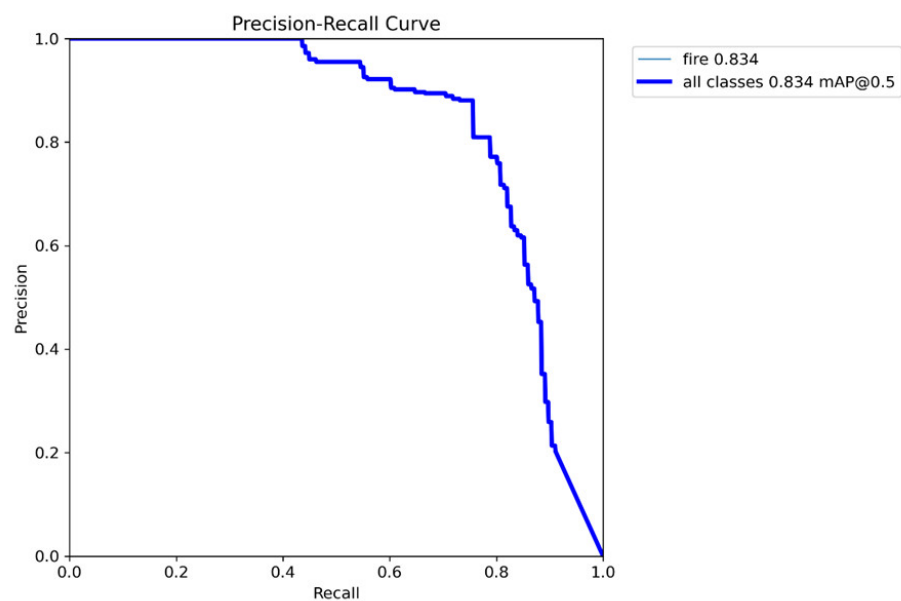


Figure 15. Model test PR curve.

The detection effect is shown in Figure 16.

It can be seen that the algorithm in this paper achieves an mAP value of 83.4% in the test set, which is able to realize the detection of smoke in the early stage of fire more accurately.

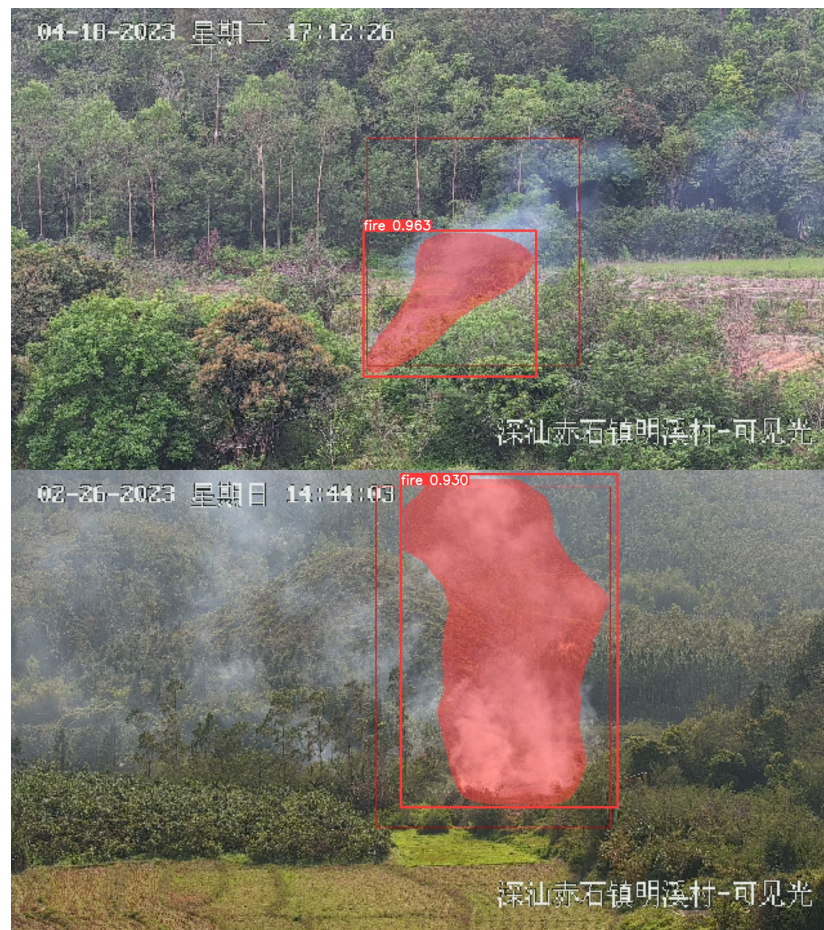


Figure 16. Fireworks images and their confidence values obtained after deep learning training.

3.3. FWI Value Calculation

Data including temperature, humidity, wind speed, wind direction, soil temperature, soil moisture content, rainfall in the last hour, consecutive days without rain, etc., can be obtained through the meteorological stations, based on which the fire risk level is calculated according to the FWI calculation formula, which serves as the basis for forest fire risk early warning aid judgment.

To eliminate the influence of the initial value and to form a complete time series, in this paper, the meteorological factors of the time series are used to carry out the calculation of each component factor of the FWI system, and the duration of this time series is more than 1 year longer than that of the data to be analyzed, and the period affected by the initial value is not included in the analytical process when carrying out the analysis, to minimize the influence of the results due to the difference in the initial value. The forest fire weather index FWI values for March are shown in Table 3.

The FWI values for March are as follows:

Table 3. Forest Fire Weather Index FWI values for March (partial).

Dates	Temp (°C)	Relative Humidity (%)	Air Velocity (m/s)	Measured Quantity of Rain (mm)	FWI Value	Fire Risk Level	Fire Danger Rating for This Article
15 March 2023 14:00	24.1	64.5	3.9	0	27.18950643	4	3
16 March 2023 13:00	25.9	48.4	5.7	0	45.56674525	5	4
17 March 2023 14:00	25.5	66.5	6.4	0	33.35758052	5	4
18 March 2023 13:00	24.3	74.9	4.3	0	22.38434888	3	3
19 March 2023 0:00	19.2	89.5	0.5	0	7.641192305	1	1
20 March 2023 14:00	26.2	67.7	4.1	0	23.98472086	3	2
21 March 2023 10:00	24.9	83.8	3	0	11.64921009	2	1

The selection of fire danger level thresholds is based on fire archives, historical fire conditions and weather realities and other adjustments to determine the historical empirical values. The fire danger thresholds of the selected picture areas are shown in Table 4:

Table 4. FWI fire risk thresholds.

Fire Risk Level	1	2	3	4	5
Fire danger rating thresholds	<10.01	≥10.01	≥17.52	≥25.03	≥32.53

3.4. Experimental Results

The accuracy, precision, recall, and F1 score were calculated to determine the performance of the experimental results obtained in this study, where TP is the number of true positives, FP is the number of false positives, FN is the number of false negatives, and TN is the number of true negatives. The first letter indicates whether the real value is correctly divided from the predicted value, T indicates that the judgment is correct, and F indicates that the judgment is wrong (false); the second letter indicates the result of the classifier's judgment (prediction), P indicates that the judgment is a positive case, and N indicates that the judgment is a negative case. The relationship between them is shown below. First, the accuracy and precision were obtained using Equations (1) and (2), the recall was obtained using Equation (3), and the reconciled mean F1 score of accuracy and detection was obtained using Equation (4)

$$\text{Accuracy} = \frac{\text{TP} + \text{TN}}{\text{TP} + \text{TN} + \text{FP} + \text{FN}} \quad (1)$$

$$\text{Precision} = \frac{\text{TP}}{\text{TP} + \text{FP}} \quad (2)$$

$$\text{Recall} = \frac{\text{TP}}{\text{TP} + \text{FN}} \quad (3)$$

$$\text{F1 Score} = 2 * \frac{\text{Precision} * \text{Recall}}{\text{Precision} + \text{Recall}} \quad (4)$$

In the judgment rule of 2.4 herein, said first threshold, second threshold, third threshold, and fourth threshold vary slightly according to environmental conditions, and the first threshold obtained from the experiments conducted herein is 90%, the second threshold is 80%, the third threshold is 65%, and the fourth threshold is 58%. Then whether or not a fire warning should be issued is determined according to the fire danger level, the confidence level of the occurrence of fire in the visible image, and the judgment result based on an infrared image. According to the evaluation index of the classification algorithm, the number of fire warnings that need to be issued and are actually fires is judged as TP, the number of fire warnings that need to be issued but are not actually fires is judged as FP, the number of fire warnings that do not need to be issued but are actually fires is judged as FN, and the number of fires that do not need to be issued but are actually not fires is judged as TN, and then the values of the accuracy, precision, recall and f1 score are calculated according to the formulas in this chapter. Table 5 shows the accuracy, precision, recall, and F1-score calculated based on the fire warning results, as well as a comparison with the method using only YOLOv5 with the EMA attention mechanism (YOLOV5-EMA) in Section 2.1 herein, and Computer Vision Detection and Convolutional Neural Network (CVD-CNN) [31], Single Shot Multibox Detector (SSD) [48] Faster R-CNN (Region proposal Convolutional Neural Network) [49] for comparison results.

Table 5. Comparison experiment.

Algorithms	Accuracy	Precision	Recall	F1 Score
The model presented	94.12	96.10	93.67	94.87
YOLOv5-EMA	83.42	80.06	80.27	80.21
CVD-CNN	93.0	93.9	92.0	92.9
SSD	85	84.3	86	85.1
Faster R-CNN	89.0	89.8	88	88.9

As shown in Table 5, the model presented in this study achieves an accuracy of 94.12%, a precision of 96.1%, a recall of 93.67, an F1-score of 94.87, and an accuracy of 83.42% using YOLOv5-EMA deep learning algorithms alone, with an accuracy of 93.0% for CVD-CNN, 85% for SSD, and 89.0% for Faster R-CNN.

4. Discussion

In this study, the object of our research is not to distinguish images with smoke from images without smoke, but rather images that contain situations such as smoke and fire, water mist, clouds, dust, exhaust from large machines, reflection of the sun, etc., that are determined by a separate type of visible or infrared image to be a forest fire, causing false alarms. The types of images that cause early warnings are shown in Table 6.

Table 6. Types of images that trigger alarms.

Alarm Image Classification	Visible Image Alarm	Infrared Image Alarm	Forest Fire Dangerrating
Mist	1	1	≥2
Water mist	1	0	1 or 2
Cloud	1	0	≥2
Dust	1	0	≥2
Large Machine Exhaust	1	1	≥2
Sun Reflection	0	1	≥2

In this study, we collect a large number of images of the early stage of forest fires, and then label these images to mark the location and shape of the fire point and the smoke and fire, and collect other visible light images that will cause false alarms of fire, including images of fog, cloud images, images of high temperatures of machines, images of reflections of lakes, images of chimneys of buildings, etc. We label the objects that cause false fire alarms as well as their location and shape, and divide them into four categories to be labeled as fire, cloud, fog, and other, and then train the predefined model using these labeled images, and ultimately obtain a deep-learning-based smoke detection model. Through deep learning training, the detection of smoke at the early stage of a fire can be more accurately realized. In addition, the smoke detection model obtained by the training method can be trained to obtain confidence in the occurrence of fire in images containing water mist, clouds, dust, the exhaust of large machines, and the reflection of the sun.

In this paper, YOLOv5 is selected for deep learning training of visible images, and the EMA (Exponential Moving Average) attention mechanism is introduced in the YOLOv5 model feature extraction network to improve the feature representation capability of the network. The computational process of the EMA attention mechanism is an existing process, and this EMA attention mechanism fully considers the feature grouping and the multi-scale structure, which is conducive to the effective establishment of short-term and long-term dependencies, thus achieving a better performance.

In forest fire monitoring scenarios, it is difficult for visible light images to distinguish smoke and fire from other shapes like clouds and machine exhaust, resulting in a high false recognition rate. This situation was improved after we combined the fire danger level obtained from the fire weather index with the infrared image warning. As can be seen from Table 6, most of the time when water mist or vapor occurs, the meteorological

environment generally shows a low temperature and high humidity, which corresponds to a fire weather level of 1 or 2, which does not trigger an infrared alarm; when dust and white clouds appear, the meteorological environment generally shows a high temperature and low humidity, which does not trigger an infrared warning. The sun's reflection and the exhaust of machines and equipment trigger an infrared warning, but their visible similarity with smoke is very low, and will not trigger a visible image warning. Therefore, in summary, we use deep learning training of light with the FWI fire danger level and infrared image warning, which has a higher accuracy than simply using visible image or infrared image warnings, further improving the precision rate and solving the problem of the high rate of false alarms at the early stage of forest fire.

5. Conclusions

This paper proposes a method for monitoring and early warning of forest fire danger, wherein the method determines the current fire danger level based on the current FWI, the confidence level of the occurrence of a fire situation in visible light images, and the result of the judgment based on infrared images to determine whether or not to issue a fire warning. The study first labels the collected visible light images, including images of the early stages of a forest fire situation and other visible light images that cause false fire alarms, such as clouds, fog, and dust, with their locations and shapes. Then the EMA attention mechanism is introduced to the feature extraction network of the YOLOv5 model to obtain the described predefined model, and the predefined model is trained by deep learning using the labeled images to obtain a deep learning-based smoke detection model. The fire danger level obtained from the fire weather index and the infrared image warning are combined on this basis, which resolves the problem of the deep smoke detection model making it difficult to distinguish fire-generated smoke from other shapes like clouds and machine exhausts in visible images. Using this method, false alarms caused by water mist, clouds, dust, etc., are effectively reduced, and the accuracy of the initial risk warning of forest fires is improved.

In our future research, we will continue to work on early risk monitoring and warning of forest fires. We plan to use visible images, infrared images, and meteorological information as parameters together, and to put them in a large model for training, to obtain a more accurate warning model, and at the same time, be able to classify interfering images such as water mist, clouds, dust, exhaust from large machines, and the reflection of the sun.

Author Contributions: Conceptualization, D.S.; Methodology, D.S.; Software, D.S.; Validation, D.S.; Formal analysis, D.S. and H.Z.; Investigation, D.S.; Resources, D.S.; Data curation, L.H., H.Z. and F.Y.; Writing—original draft, D.S. and H.Z.; Writing—review & editing, D.S. and H.Z.; Visualization, H.Z.; Supervision, F.Z. and D.Y.; Project administration, F.Z., D.Y. and H.Z. All authors have read and agreed to the published version of the manuscript.

Funding: This research was supported by a grant (61973209) of National Natural Science Foundation of China.

Institutional Review Board Statement: Not applicable.

Informed Consent Statement: Not applicable.

Data Availability Statement: The original contributions presented in the study are included in the article, further inquiries can be directed to the corresponding author.

Conflicts of Interest: The authors declare no conflict of interest.

References

1. Vicente, J.; Guillemant, P. An image processing technique for automatically detecting forest fire. *Int. J. Therm. Sci.* **2002**, *41*, 1113–1120. [[CrossRef](#)]
2. Guillemant, P. Real-time identification of smoke images by clustering motions on a fractal curve with a temporal embedding method. *Opt. Eng.* **2001**, *40*, 554–563. [[CrossRef](#)]

3. Gomez-Rodriguez, F.; Arrue, B.C.; Ollero, A. *Smoke Monitoring and Measurement Using Image Processing: Application to Forest Fires*; Automatic Target Recognition XIII SPIE: Orlando, FL, USA, 2003; Volume 5094, pp. 404–411.
4. Fernandes, A.M.; Utkin, A.B.; Lavrov, A.V.; Vilar, R.M. Neural Network Based Recognition of Smoke Signatures from Lidar Signals. *Neural Process. Lett.* **2004**, *19*, 175–189. [[CrossRef](#)]
5. Jakovčević, T.; Stipaničev, D.; Krstinić, D. Visual spatial-context based wildfire smoke sensor. *Mach. Vis. Appl.* **2013**, *24*, 707–719. [[CrossRef](#)]
6. Park, J.; Ko, B.; Nam, J.; Kwak, S. Wildfire smoke detection using spatiotemporal bag-of-features of smoke. In Proceedings of the IEEE Workshop on Applications of Computer Vision (WACV 2013), Clearwater Beach, FL, USA, 15–17 January 2013; pp. 200–205.
7. Gupta, T.; Liu, H.; Bhanu, B. Early wildfire smoke detection in videos. In Proceedings of the 2020 25th International Conference on Pattern Recognition (ICPR), Milano, Italy, 10–15 January 2021; pp. 8523–8530.
8. Áhlén, J. Smoke and fog classification in forest monitoring using high spatial resolution images. In Proceedings of the 22nd International Multidisciplinary Scientific GeoConference SGEM 2022, Albena, Bulgaria, 4–10 July 2022; pp. 131–138.
9. Sun, X.; Sun, L.; Liu, Y.; Huang, Y. Research of Forest Fire Smoke Recognition Method Based on Gray Bit Plane Technology. *Int. J. SmartHome* **2015**, *9*, 57–64. [[CrossRef](#)]
10. Zhou, Z.; Shi, Y.; Gao, Z.; Li, S. Wildfire smoke detection based on local extremal region segmentation and surveillance. *Fire Saf. J.* **2016**, *85*, 50–58. [[CrossRef](#)]
11. Wu, X.; Lu, X.; Leung, H. Video smoke separation and detection via sparse representation. *Neurocomputing* **2019**, *360*, 61–74. [[CrossRef](#)]
12. Wu, X.; Cao, Y.; Lu, X.; Leung, H. Patchwise dictionary learning for video forest fire smoke detection in wavelet domain. *Neural Comput. Appl.* **2021**, *33*, 7965–7977. [[CrossRef](#)]
13. Wu, X.; Lu, X.; Leung, H. A motion and lightness saliency approach for forest smoke segmentation and detection. *Multimed. Tools Appl.* **2020**, *79*, 69–88. [[CrossRef](#)]
14. Jia, Y.; Yang, W.; Wang, M.; Liu, L.; Zhang, D.; Qi, X. Video smoke detection with domain knowledge and transfer learning from deep convolutional neural networks. *Optik* **2021**, *240*, 166947. [[CrossRef](#)]
15. Pundir, A.S.; Raman, B. Deep Belief Network for Smoke Detection. *Fire Technol.* **2017**, *53*, 1943–1960. [[CrossRef](#)]
16. Kaabi, R.; Sayadi, M.; Bouchouicha, M.; Fnaiech, F.; Moreau, E.; Ginoux, J.M. Early smoke detection of forest wildfire video using deep belief network. In Proceedings of the 2018 4th International Conference on Advanced Technologies for Signal and Image Processing (ATSIP), Sousse, Tunisia, 21–24 March 2018; pp. 1–6.
17. Kaabi, R.; Bouchouicha, M.; Mouelhi, A.; Sayadi, M.; Moreau, E. An Efficient Smoke Detection Algorithm Based on Deep Belief Network Classifier Using Energy and Intensity Features. *Electronics* **2020**, *9*, 1390. [[CrossRef](#)]
18. Avula, S.; Badri, S.; Reddy, G. A novel forest fire detection system using fuzzy entropy optimized thresholding and STN-based CNN. In Proceedings of the 2020 International Conference on Communication Systems & NETWORKS (COMSNETS), Bangalore, India, 7–11 January 2020; pp. 750–755.
19. Zulkarnain, J.; Pahlevi, M.; Astica, Y.; Pangestuti, W.; Kusrini, K. Fire Detection based on Smoke Image using Convolutional Neural Network (CNN). In Proceedings of the 2022 4th International Conference on Cybernetics and Intelligent System (ICORIS), Prapat, Indonesia, 8–9 October 2022; pp. 1–5.
20. Sun, X.; Sun, L.; Huang, Y. Forest fire smoke recognition based on convolutional neural network. *J. For. Res.* **2021**, *32*, 1921–1927. [[CrossRef](#)]
21. Zhang, Q.; Lin, G.; Zhang, Y.; Xu, G.; Wang, J. Wildland Forest Fire Smoke Detection Based on Faster R-CNN using Synthetic Smoke Images. *Procedia Eng.* **2018**, *211*, 441–446. [[CrossRef](#)]
22. Wang, Y.; Liu, X.; Li, M.; Di, W.; Wang, L. Deep convolution and correlated manifold embedded distribution alignment for forest fire smoke prediction. *Comput. Inform.* **2020**, *39*, 318–339. [[CrossRef](#)]
23. Zhao, E.; Liu, Y.; Zhang, J.; Tian, Y. Forest Fire Smoke Recognition Based on Anchor Box Adaptive Generation Method. *Electronics* **2021**, *10*, 566. [[CrossRef](#)]
24. Mahmoud, M.; Ren, H. Forest fire detection and identification using image processing and SVM. *J. Inf. Process. Syst.* **2019**, *15*, 159–168.
25. Amaral, B.; Niknejad, M.; Barata, C. Weakly Supervised Fire and Smoke Segmentation in Forest Images with CAM and CRF. In Proceedings of the 2022 26th International Conference on Pattern Recognition (ICPR), Montreal, QC, Canada, 21–25 August 2022; pp. 442–448.
26. Cao, Y.; Yang, F.; Tang, Q.; Lu, X. An Attention Enhanced Bidirectional LSTM for Early Forest Fire Smoke Recognition. *IEEE Access* **2019**, *7*, 154732–154742. [[CrossRef](#)]
27. Wu, X.; Lu, X.; Leung, H. A video based fire smoke detection using robust AdaBoost. *Sensors* **2018**, *18*, 3780. [[CrossRef](#)]
28. Xu, G. Research on Depth Domain Adaptation and Saliency Detection Methods in Fire and Smoke Image Recognition. Ph.D. Thesis, University of Science and Technology of China, Hefei, China, 2020.
29. Luo, S.; Yan, C.; Wu, K.; Zheng, J. Smoke detection based on condensed image. *Fire Saf. J.* **2015**, *75*, 23–35. [[CrossRef](#)]
30. He, L.; Gong, X.; Zhang, S.; Wang, L.; Li, F. Efficient attention based deep fusion CNN for smoke detection in fog environment. *Neurocomputing* **2021**, *434*, 224–238. [[CrossRef](#)]
31. Ryu, J.; Kwak, D. A study on a complex flame and smoke detection method using computer vision detection and convolutional neural network. *Fire* **2022**, *15*, 108. [[CrossRef](#)]

32. Celik, T.; Demirel, H.; Ozkaramanli, H.; Uyguroglu, M. Fire detection using statistical color model in video sequences. *J. Vis. Commun. Image Represent.* **2007**, *18*, 176–185. [[CrossRef](#)]
33. Habiboğlu, Y.; Günay, O.; Çetin, A. Covariance matrix-based fire and flame detection method in video. *Mach. Vis. Appl.* **2012**, *23*, 1103–1113. [[CrossRef](#)]
34. Tan, Y.; Xie, L.; Feng, H.; Peng, L.; Zhang, Z. Flame Detection Algorithm Based on Image Processing Technology. *Laser Optoelectron. Prog.* **2019**, *56*, 161012.
35. Sun, X. Research on Forest Fire Video Recognition Technology Based on Edge Computing. Ph.D. Thesis, Northeast Forestry University, Harbin, China, 2020.
36. Wu, X. Research on Forest Smoke and Fire Detection Method Based on Video Images. Ph.D. Thesis, Southeast University, Nanjing, China, 2020.
37. Dai, P.; Zhang, Q.; Lin, G.; Shafique, M.M.; Huo, Y.; Tu, R.; Zhang, Y. Multi-scale video flame detection for early fire warning based on deep learning. *Front. Energy Res.* **2022**, *10*, 848754. [[CrossRef](#)]
38. Ciprián-Sánchez, J.; Ochoa-Ruiz, G.; Gonzalez-Mendoza, M.; Rossi, L. FIRE-GAN: A novel deep learning-based infrared-visible fusion method for wildfire imagery. *Neural Comput. Appl.* **2021**, *35*, 18201–18213. [[CrossRef](#)]
39. Sun, F.; Yang, Y.; Lin, C.; Liu, Z.; Chi, L. Forest Fire Compound Feature Monitoring Technology Based on Infrared and Visible Binocular Vision. *J. Phys. Conf. Ser.* **2020**, *1792*, 012022. [[CrossRef](#)]
40. Zhou, Z.; Wang, B.; Li, S.; Dong, M. Perceptual fusion of infrared and visible images through a hybrid multi-scale decomposition with Gaussian and bilateral filters. *Inf. Fusion* **2016**, *30*, 15–26. [[CrossRef](#)]
41. Wang, B.; Zou, Y.; Zhang, L.; Li, Y.; Chen, Q.; Zuo, C. Multimodal super-resolution reconstruction of infrared and visible images via deep learning. *Opt. Lasers Eng.* **2022**, *156*, 107078. [[CrossRef](#)]
42. Wu, X.; Wen, C.; Wang, Z.; Liu, W.; Yang, J. A novel ensemble-learning-based convolution neural network for handling imbalanced data. *Cogn. Comput.* **2023**, *16*, 177–190. [[CrossRef](#)]
43. Zhang, R.; Wen, C. Sod-Yolo: A small target defect detection algorithm for wind turbine blades based on improved Yolov5. *Adv. Theory Simul.* **2022**, *5*, 2100631. [[CrossRef](#)]
44. Ouyang, D.L.; He, S.; Zhang, G.; Luo, M.; Guo, H.; Zhan, J.; Huang, Z. Efficient Multi-Scale AttentionModule with Cross-Spatial Learning. In Proceedings of the IEEE International Conference on Acoustics Speech and Signal Processing (ICASSP 2023), Rhodes Island, Greece, 4–10 June 2023; pp. 1–5.
45. Tian, X.; Zhang, Y. Review of forest fire danger level forecasting systems. *World For. Res.* **2006**, *19*, 39–46.
46. Van Wagner, C.E.; Pickett, T.L. *Equations and FORTRAN Program for the Canadian Forest Fire Weather Index System*; Forestry Technical Report 33; Canadian Forestry Service: Ottawa, ON, Canada, 1985.
47. Van, W. *Structure of the Canadian Forest Fire Weather Index*; Environment Canada, Forestry Service: Alberta, Canada, 1974.
48. Liu, W.; Anguelov, D.; Erhan, D.; Szegedy, C.; Reed, S.; Fu, C.-Y.; Berg, A.C. SSD: Single shot multibox detector. In *Computer Vision-ECCV 2016*; Springer: Cham, Switzerland, 2016; pp. 21–37.
49. Ren, S.; He, K.; Girshick, R.; Sun, J. Faster R-CNN: Towards real-time object detection with region proposal networks. *IEEE Trans. Pattern Anal. Mach. Intell.* **2017**, *39*, 1137–1149. [[CrossRef](#)]

Disclaimer/Publisher’s Note: The statements, opinions and data contained in all publications are solely those of the individual author(s) and contributor(s) and not of MDPI and/or the editor(s). MDPI and/or the editor(s) disclaim responsibility for any injury to people or property resulting from any ideas, methods, instructions or products referred to in the content.